

Electronic Supplementary Information

Polymorphism of human telomeric quadruplexes with drugs: A multi-technique biophysical study

L. Comez^{1*}, F. Bianchi², V. Libera², M. Longo³, C. Petrillo², F. Sacchetti², F. Sebastiani⁴, F. D'Amico⁵, B. Rossi⁵, A. Gessini⁵, C. Masciovecchio⁵, H. Amenitsch⁶, C. Sissi⁷, A. Paciaroni^{2*}

¹*IOM-CNR c/o Dipartimento di Fisica e Geologia, Università di Perugia, 06123 Perugia, Italy*

²*Dipartimento di Fisica e Geologia, Università di Perugia, 06123 Perugia, Italy*

³*JCNS Forschungszentrum Jülich GmbH at Heinz Maier-Leibnitz Zentrum (MLZ), 85748 Garching, Germany*

⁴*Dipartimento di Chimica "Ugo Schiff", Università degli Studi di Firenze, 50019 Sesto Fiorentino (FI), Italy*

⁵*Elettra Synchrotron Light Laboratory, S.S. 14 Km 163.5, 34012 Trieste, Italy*

⁶*Institute of Inorganic Chemistry, Graz University of Technology, 8010 Graz, Austria*

⁷*Dipartimento di Scienze del Farmaco, Via Marzolo 5, 35131 Padova, Italy*

*corresponds to: comez@iom.cnr.it, alessandro.paciaroni@unipg.it

Contents:

Circular dichroism

Figure S1 contains single-wavelength melting profiles of Tel22, Tel22-Ber and Tel22-Palm and corresponding derivative curves.

Table S1 contains the thermodynamics parameters for the thermal melting of Tel22 and Tel22-Ber, and Tel22-Palm, obtained from SVD analysis on CD data

Ultraviolet Resonant Raman Scattering

Figure S2 gives UVRR and DS spectra for sample Tel22 during a 30 – 90 °C temperature scan.

Figure S3 gives UVRR and DS spectra for sample Tel22-Ber during a 30 – 90 °C temperature scan.

Figure S4 gives UVRR and DS spectra for sample Tel22-Palm during a 30 – 90 °C temperature scan.

Figure S5 reports the intensity of the DS spectra as a function of temperature.

Figure S6 reports the experimental and theoretical Raman spectrum of Tel22-Palm at ambient temperature, as an example of the fitting procedure.

Figure S7 reports the global simultaneous fitting procedure by using a two-step law on a selection of Tel22 vibrational peaks.

Figure S8 reports the global simultaneous fitting procedure by using a two-step law on a selection of Tel22-Ber vibrational peaks.

Figure S9 reports the global simultaneous fitting procedure by using a two-step law on a selection of Tel22-Palm vibrational peaks.

Table S2 contains the results from the global simultaneous fitting procedure on the relative intensity of selected vibrational peaks.

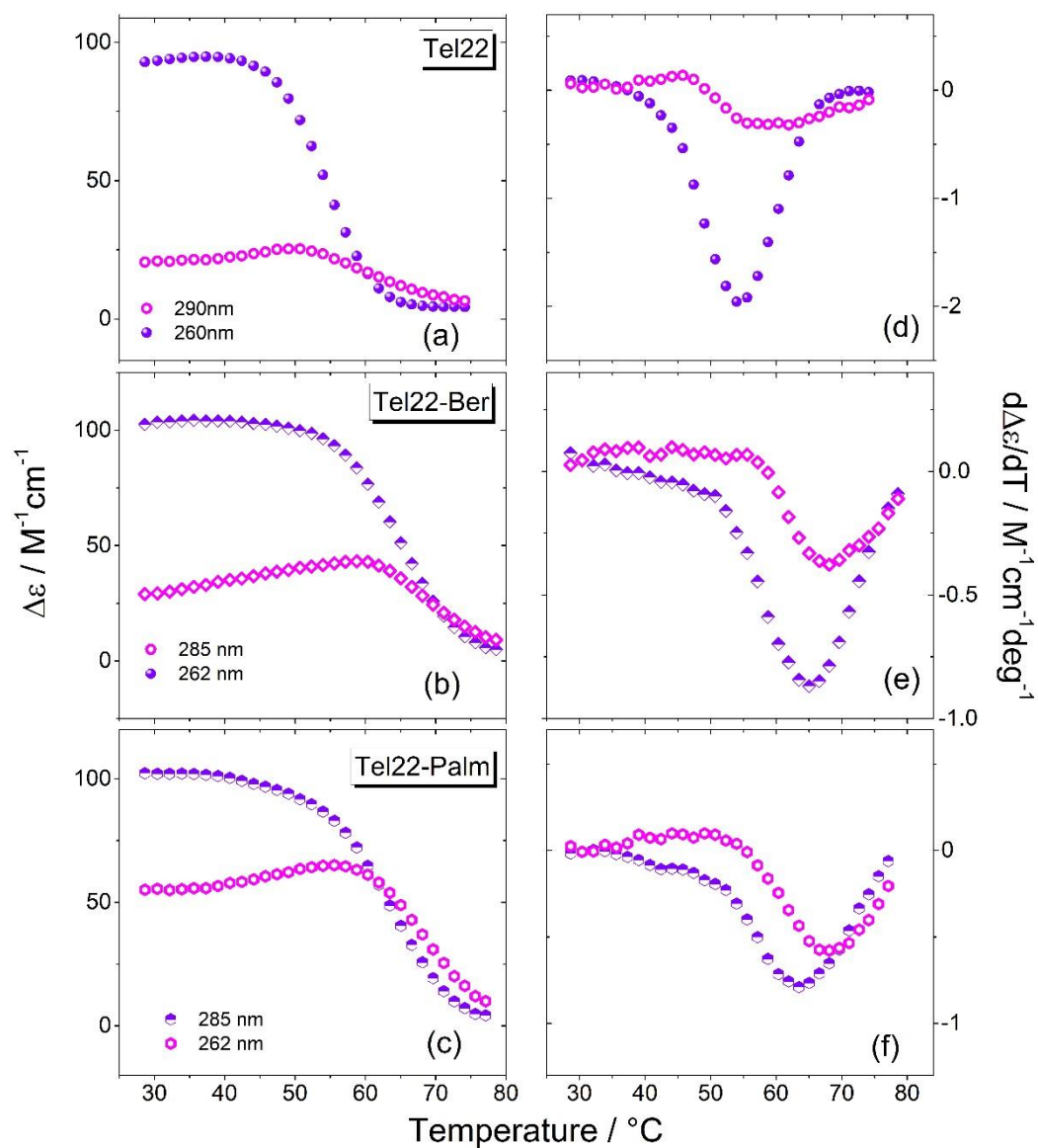


Figure S1. Single-wavelength melting profiles of Tel22, Tel22-Ber and Tel22-Palm extracted, at the indicated selected wavelengths, from the experimental CD data set. The CD curves taken at different wavelengths display different temperature dependence. Panels (d), (e) and (f) represent the first derivative of melting profiles curves in (a), (b) and (c), respectively. All these trends represent a signature of the presence of intermediate states along the thermal unfolding path [S1].

	Tel22	Tel22-Ber	Tel22-Palm
T_{m1} (°C)	43.0±0.9	40.0±0.8	42.3±0.5
T_{m2} (°C)	58.0±0.8	61.9±0.8	61.7±1.8
T_{m3} (°C)	63.0±0.5	70.1±0.5	69.2±0.8
ΔH_1 (kcal·mol ⁻¹)	-30±3	-21.9±1.8	-21.0±3.5
ΔH_2 (kcal·mol ⁻¹)	-34±3	-52.3±4.4	-40.6±3.4
ΔH_3 (kcal·mol ⁻¹)	-40±4	-73.8±3.5	-69.4±8.4
ΔS_1 (kcal·mol ⁻¹ K ⁻¹)	-0.095±0.009	-0.070±0.006	-0.067±0.010
ΔS_2 (kcal·mol ⁻¹ K ⁻¹)	-0.103±0.009	-0.156±0.013	-0.121±0.011
ΔS_3 (kcal·mol ⁻¹ K ⁻¹)	-0.119±0.012	-0.215±0.010	-0.203±0.025
ΔG_1^* (kcal·mol ⁻¹)	-1.7±0.4	-1.04±0.45	-1.2±0.9
ΔG_2^* (kcal·mol ⁻¹)	-3.4±0.8	-5.8±0.8	-4.5±0.8
ΔG_3^* (kcal·mol ⁻¹)	-4.5±0.9	-9.7±0.9	-8.9±0.9
ΔH_{TOT} (kcal·mol ⁻¹)	-104±6	-148±6	-131±10
ΔS_{TOT} (kcal·mol ⁻¹ K ⁻¹)	-0.32±0.02	-0.44±0.02	-0.39±0.023
ΔG_{TOT} (kcal·mol ⁻¹)	-9.6±1.3	-16.5±1.3	-14.6±1.5
$\Delta\Delta H$ (kcal·mol ⁻¹)		-44±8	-27±11
$\Delta\Delta G$ (kcal·mol ⁻¹)		-7±2	-5±2

Table S1. Thermodynamics parameters for the thermal melting of Tel22 and Tel22-Ber, and Tel22-Palm, obtained from SVD analysis on CD data. ΔG_1^* , ΔG_2^* and ΔG_3^* are calculated at T=25°C. The errors on ΔG are determined as reported in Ref. [S2].

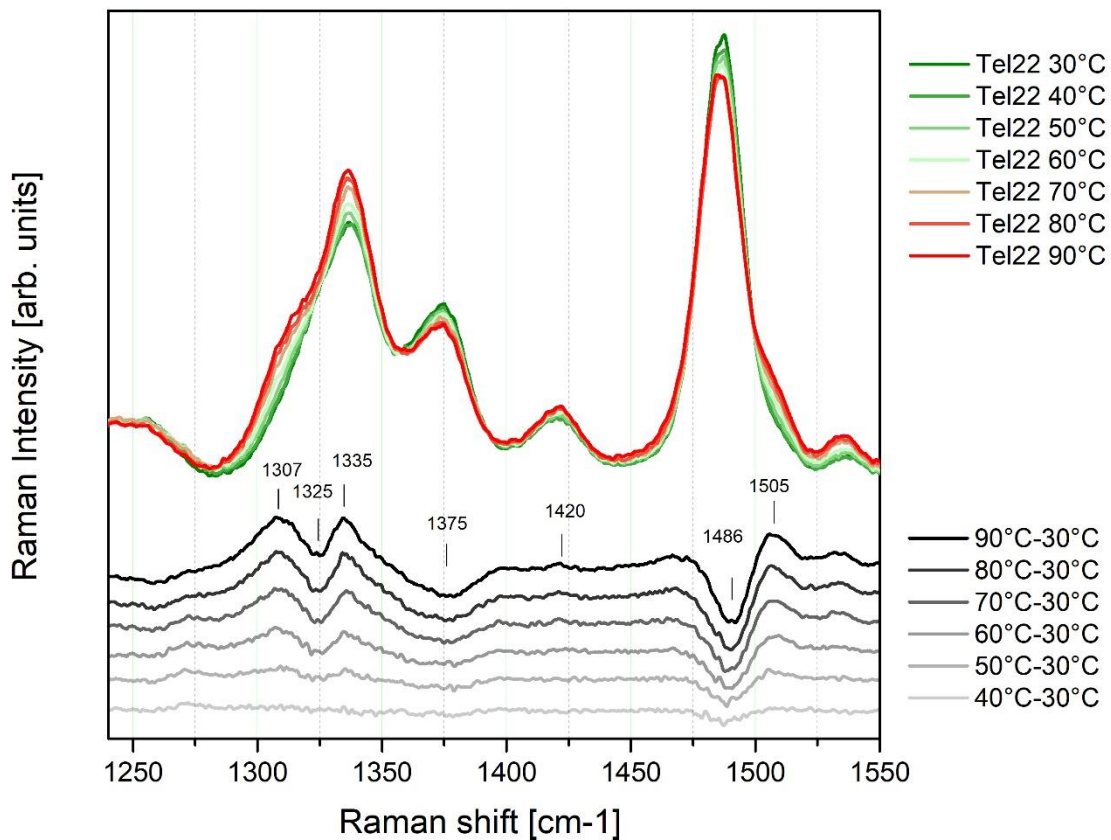


Figure S2. Raman spectra for sample Tel22 during a 30 – 90 °C temperature scan. Difference spectra (DS) are also shown according to the sequence reported in the legend.

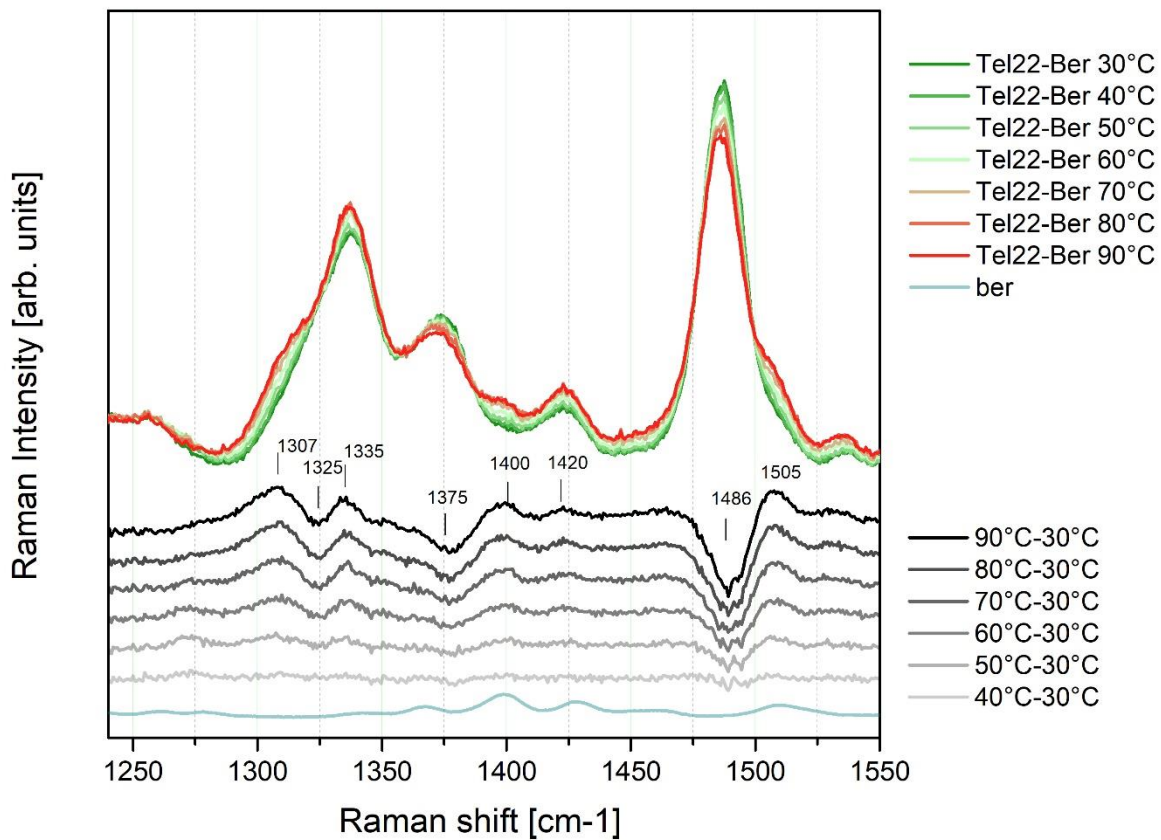


Figure S3. Raman spectra for sample Tel22-Ber during a 30 – 90 °C temperature scan. Difference spectra (DS) and the berberine Raman spectra collected at the room temperature are also shown in the figure as indicated in the legend.

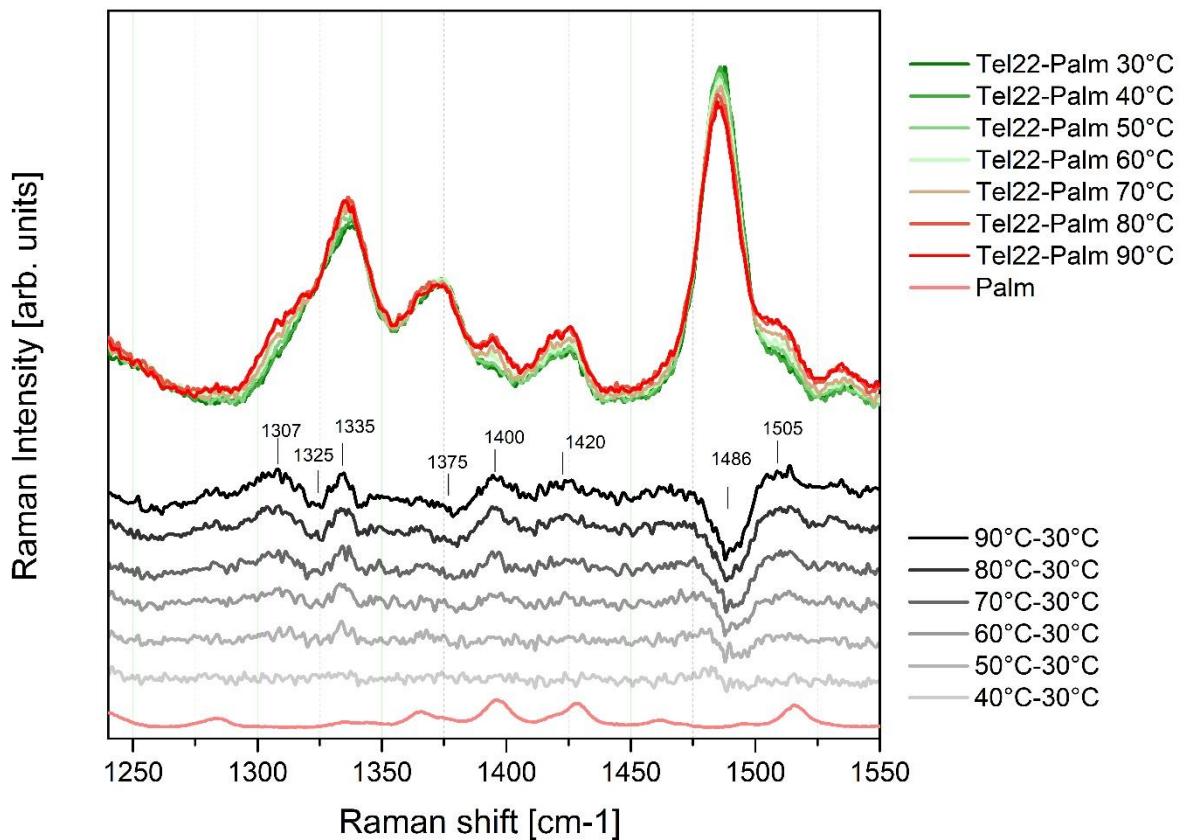


Figure S4. Raman spectra for sample Tel22-Palm during a 30 – 90 °C temperature scan. Difference spectra (DS) and the palmatine Raman spectra collected at the room temperature are also reported in the figure as indicated in the legend.

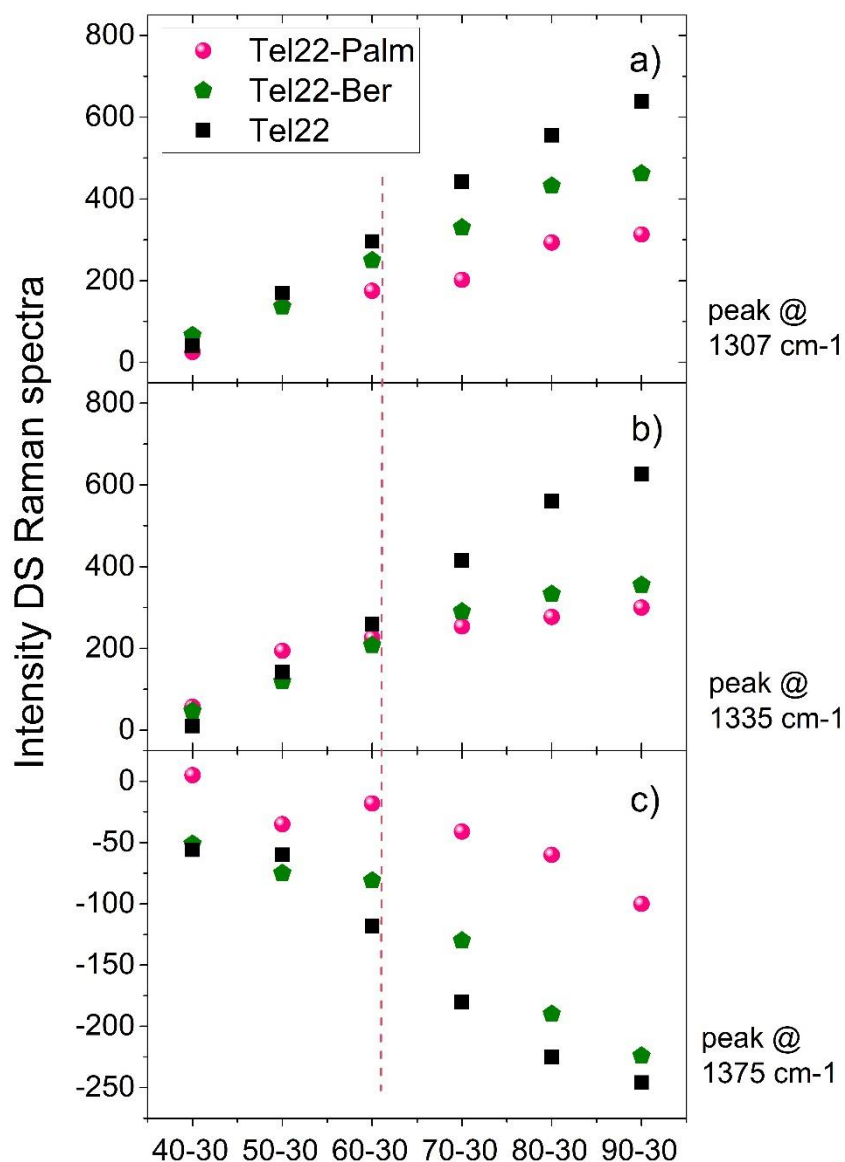


Figure S5. Intensity of the DS spectra as a function of temperature for the representative residual peaks centered at around 1307, 1335 and 1375 cm^{-1} , respectively. It is clear that above the temperature corresponding to the passage from the first to the second intermediate state, the differences between the three systems intensify, particularly for the case of the Tel22-Palm in which it is observed, from CD, an inversion (H vs P) between the most populated states.

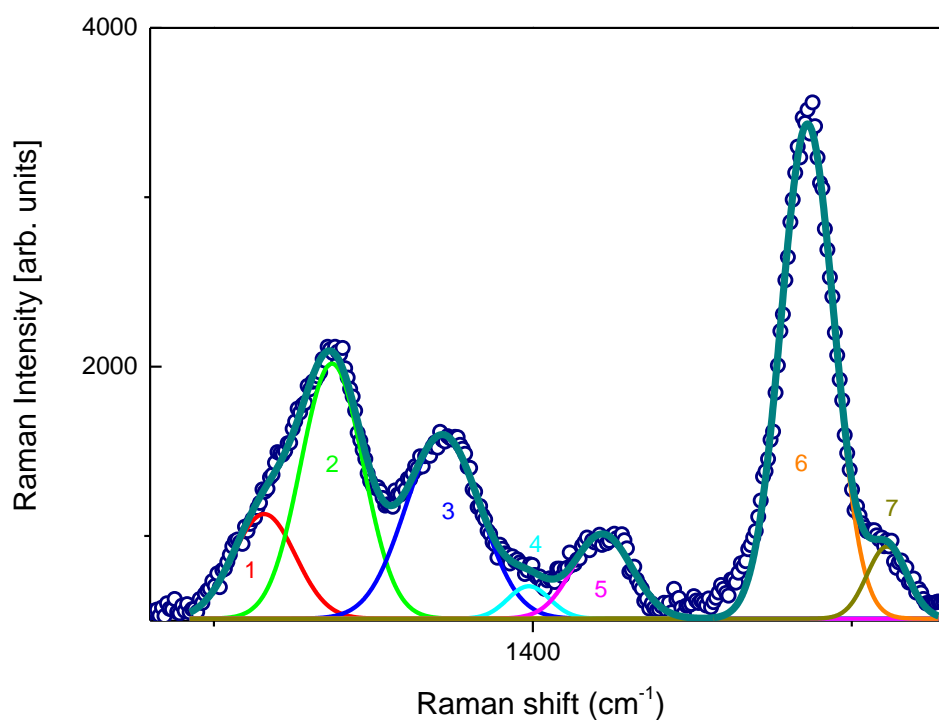


Figure S6. Experimental and theoretical Raman spectrum of Tel22-Palm at ambient temperature. Data analysis was performed using the minimum number (7) of gaussian functions. The cumulative fitting curve together with the single components are shown to visualize the corresponding Raman vibrations. Peaks from 1 to 7 on increasing frequency, are centered at about 1316, 1337, 1372, 1400, 1422, 1486, 1511 cm⁻¹. These positions may differ by some cm⁻¹ depending on the environmental sample conditions, and the assignments of the the group bands for human telomeres is reported in Refs. [S3, S4].

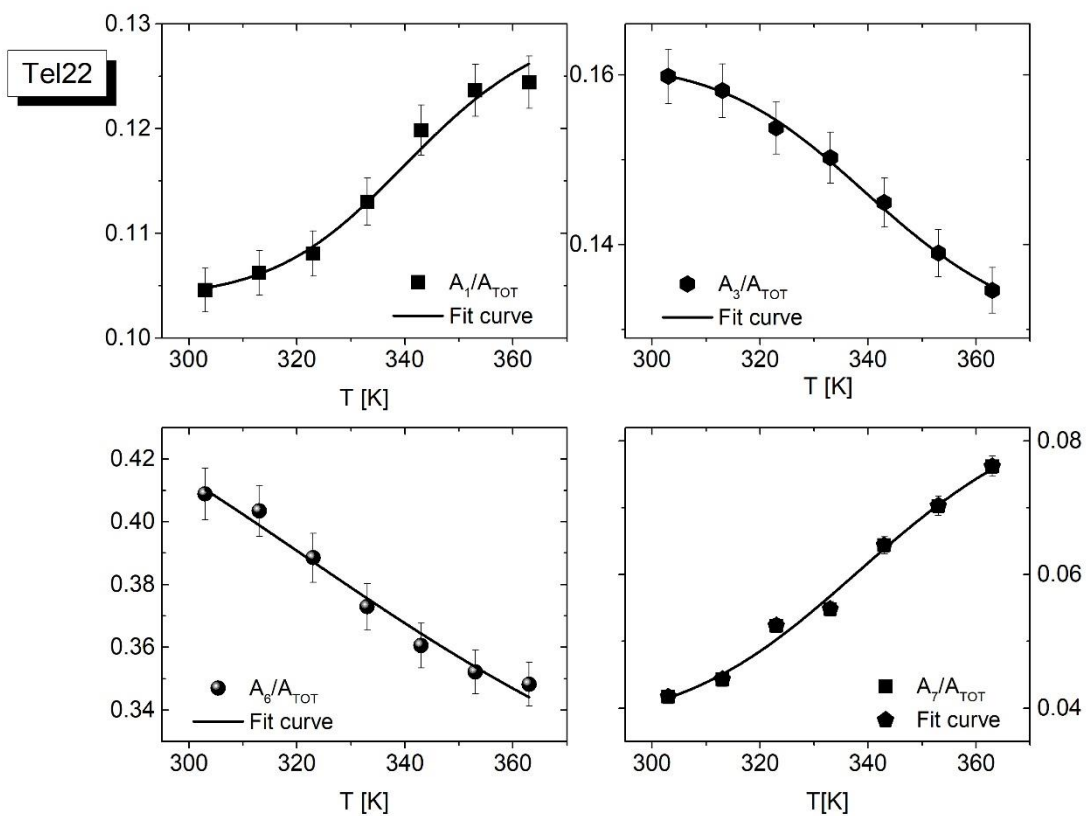


Figure S7 Global simultaneous fitting procedure by using the two-step law of eq. S1 on the relative intensity of peaks labelled as 1, 3, 6, and 7 (see Fig. S6) for Tel22: a unique melting temperature is able to reproduce all the experimental trends. The results of the data analysis is reported in Table S2.

$$A_{vib} = \frac{A_F + A_U \exp\left(\frac{\Delta H_{vib}}{R} \left(\frac{1}{T_m} - \frac{1}{T}\right)\right)}{1 + \exp\left(\frac{\Delta H_{vib}}{R} \left(\frac{1}{T_m} - \frac{1}{T}\right)\right)} \quad \text{Eq [S1]}$$

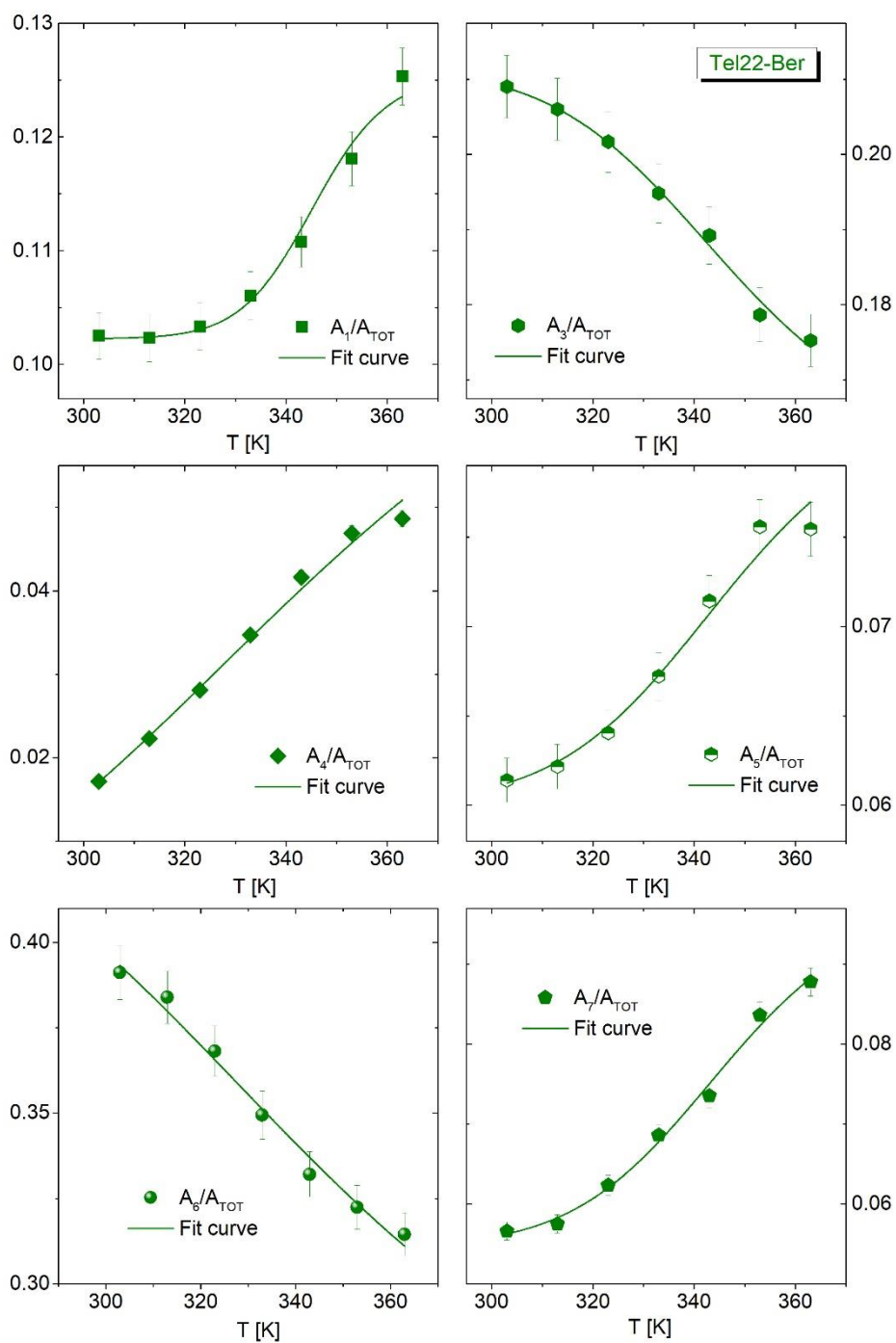


Figure S8 Global simultaneous fitting procedure by using the two-step law of eq. S1 on the relative intensity of peaks labelled as 1, 3, 4, 5, 6, and 7 (see Fig. S6) for Tel22-Ber: a unique melting temperature is able to reproduce all the experimental trends. The results of the data analysis is reported in Table S2.

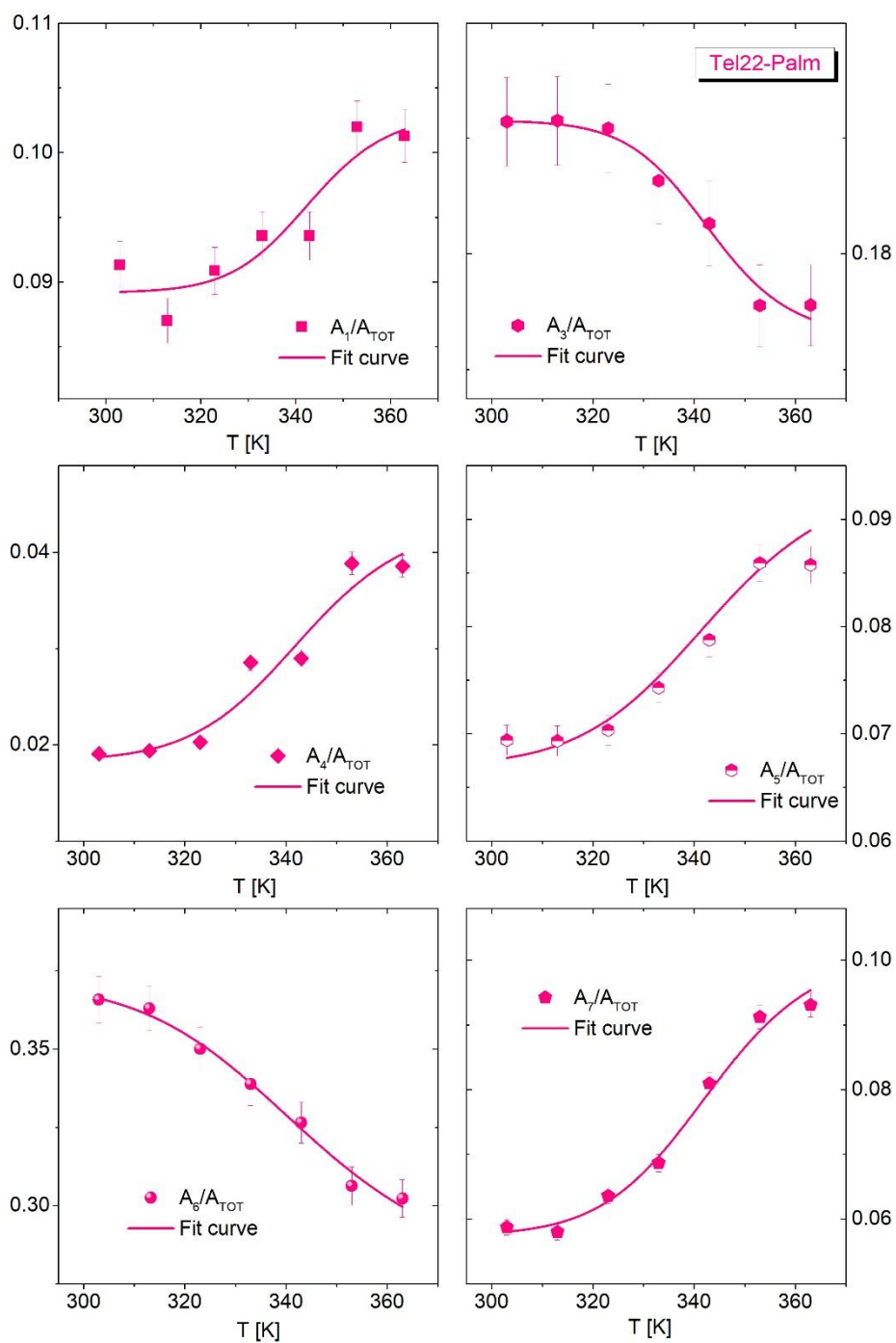


Figure S9 Global simultaneous fitting procedure by using the two-step law of eq.S1 on the relative intensity of peaks labelled as 1, 3, 4, 5, 6, and 7 (see Fig. S6) for Tel22-Palm: a unique melting temperature is able to reproduce all the experimental trends. The results of the data analysis is reported in Table S2.

	T _m (°C)	ΔH _{vib1} (Kcal/mol)	ΔH _{vib3} (Kcal/mol)	ΔH _{vib4} (Kcal/mol)	ΔH _{vib5} (Kcal/mol)	ΔH _{vib6} (Kcal/mol)	ΔH _{vib7} (Kcal/mol)
Tel22	68±5	-17.7±0.9	15.8±0.8		-	5.3±0.3	-12.6±0.6
Tel22-Ber	72.4±3.5	-32.7±1.6	14.0±0.7	-5.7±0.3	-14.5±0.7	9.3±0.5	-16.0±0.8
Tel22-Palm	70.0±3.7	-27.3±1.4	28.8±1.4	-21.5±1.1	-18.2±0.9	14.8±0.8	-21.8±1.1

Table S2 Results from the global simultaneous fitting procedure on the relative intensity of peaks labelled as 1, 3, 6, and 7 for Tel22 (see Fig. S6), and 1, 3, 4, 5, 6, and 7 for Tel22-Ber and Tel22-Palm (see Fig. S7-Fig. S8).

References

- [S1] R. D. Gray, R. Buscaglia, and J. B. Chaires, *J. Am. Chem.Soc.* 2012, **134**, 16834–16844.
[S2] H.A. Saroff, *Biochem.* 1989, **176**, 161.
[S3] J. Palacký, P. Mojzeš, I. Kejnovská, and M. Vorlíčková, *J Raman Spectrosc.* 2019; **51**, 301-312.
[S4] S. Di Fonzo, C. Bottari, J. W. Brady, L. Tavagnacco, M. Caterino, L. Petraccone, J. Amato, C. Giancola and A. Cesàro, *Phys. Chem. Chem. Phys.*, 2019, **21**, 2093-2101.